RESEARCH ARTICLE-CHEMISTRY

Preparation, Characterization and Adsorption Study of PEDGE-Cross-linked Magnetic Chitosan (PEDGE-MCh) Microspheres for Cd^{2+} Removal

Rahmi Rahmi[1] · Lelifajri Lelifajri[1] · Mudassar Iqbal[2] · Fathurrahmi Fathurrahmi[1] · Jalaluddin Jalaluddin[3] · Rahmawati Sembiring[1] · Mutia Farida[4] · Muhammad Iqhrammullah[1,5]

Abstract

To enhance the ability and practicality of chitosan used for wastewater treatment, this study aimed to modify chitosan through cross-linking and addition of magnetic properties. Cross-linked magnetic chitosan microspheres were prepared using the inverse phase dispersion method and then applied for Cd^{2+} removal from water. Fe$_3$O$_4$ nanoparticles prepared from local iron sand were embedded with chitosan cross-linked by polyethylene glycol diglycidyl ether (PEDGE) to produce PEDGE cross-linked magnetic chitosan (PEDGE-MCh) microspheres. PEDGE-MCh microspheres were characterized by Fourier transform infrared, scanning electron microscopy energy-dispersive X-ray spectroscopy, and X-ray diffraction analyses. Altogether, the characterization confirmed the formation of cross-linking and the interaction among components in the adsorbent. Additionally, the characterization also revealed the additional features of functional groups, rougher surface, and more amorphous properties beneficial in pollutant removal. Further, the batch adsorption experiments suggest that the cross-linking and addition of Fe$_3$O$_4$ improved the adsorption capacity. The highest adsorption capacity was obtained at pH 5 with a contact time of 40 min. Adsorption isotherm studies indicated that the Cd^{2+} adsorption onto PEDGE-MCh microsphere was Redlich-Peterson dependent (R^2 = 0.9996 and root-mean-square errors = 0.064). The regeneration remained the primary challenge of PEDGE-MCh application in the wastewater treatment.

Keywords Iron oxide · Adsorptive removal · Isotherm · Biopolymer · Cross-linking

1 Introduction

Chitosan is a biopolymer produced from deacetylation process of chitin using alkaline [1, 2]. Chitosan is widely used in various industries such as health, cosmetics, agriculture, livestock and paper industries [3–6]. Recently, chitosan has gained a spotlight as an emerging adsorbent material for

✉ Rahmi Rahmi
rahmi@fmipa.unsyiah.ac.id

Lelifajri Lelifajri
lelifajri@chem.unsyiah.ac.id

Mudassar Iqbal
mudassariqbal@aup.edu.pk

Fathurrahmi Fathurrahmi
fathurrahmi@unsyiah.ac.id

Jalaluddin Jalaluddin
jalaluddinyunus@unsyiah.ac.id

Rahmawati Sembiring
rahmawati.sembiring@mhs.unsyiah.ac.id

Mutia Farida
tyamutya91@gmail.com

Muhammad Iqhrammullah
m.iqhram@oia.unsyiah.ac.id

[1] Department of Chemistry, Universitas Syiah Kuala, Darussalam, Banda Aceh 2311, Indonesia

[2] Department of Agricultural Chemistry, The University of Agriculture, Peshawar 25120, Pakistan

[3] Mechanical Engineering Department, Universitas Syiah Kuala, Darussalam, Banda Aceh 23111, Indonesia

[4] Department of Chemistry Education, Faculty of Tarbiyah and Teaching, Universitas Islam Negeri Ar-Raniry, Banda Aceh 23111, Indonesia

[5] Graduate School of Mathematics and Applied Sciences, Universitas Syiah Kuala, Banda Aceh 23111, Indonesia

🖄 Springer

industrial wastewater treatment [7], including in removing notorious heavy metal from the water [8, 9]. Chitosan possesses both N- and O-containing functional groups which are useful in forming interaction with the heavy metal, either through complexation or electratostatic interaction [10, 11]. As an adsorbent, chitosan has some advantages, such as non-toxic, biodegradable, and abundant availability. However, chitosan in pure form has certain limitations, including high solubility at low pH levels and weak mechanical properties. In addition, chitosan is usually used as a powder adsorbent and its size makes it very difficult to separate from the solution after the adsorption process. Therefore, this study aimed to improve the chitosan through modifications to enhance its usage as an adsorbent.

Some researchers have reported chitosan modifications using a cross-linking agent to improve chitosan stability in acidic solutions [12]. The most common cross-linking agent of chitosan is glutaraldehyde [13–16]. However, glutaraldehyde is toxic and consumes the NH_2 groups of chitosan during the cross-linking (aldehyde reacts with an amine). The lost of NH_2 could contribute to low adsorption efficiency, since it is the primary binding site for metal ions. Therefore, a non-toxic cross-linking agent, namely polyethylene glycol diglycidyl ether (PEDGE), was used in this work. PEDGE forms a cross-linking network of chitosan by reacting with hydroxyl group (OH).

Herein, we embedded the PEDGE-cross-linked chitosan with magnetic iron oxide (Fe_3O_4) particles to ease the separation of adsorbent from the reactor, as conducted by multiple studies [8, 17–19]. Most studies, however, used commercial Fe_3O_4 for magnetic chitosan preparation [20, 21]. The commercial iron oxide is expensive, resulting in a high-cost adsorbent. Whereas, in this research, the Fe_3O_4 separated from local iron sand and readily available in Aceh, Indonesia, was used. This study also performed characterization using X-ray diffraction (XRD), Fourier transform infrared (FT-IR), and scanning electron microscopy—energy-dispersive X-ray spectroscopy (SEM-EDS) analysis. The adsorption capacity of PEDGE-MCh microspheres was examined for Cd^{2+} removal from water with various contact times, pH, and initial concentrations of Cd^{2+}. The novelty of this study is derived from the modification of chitosan beads using PEDGE and natural Fe_3O_4, in which to the best of our knowledge, it has never been reported before.

2 Materials and Methods

2.1 Materials

Chemicals used in this study were PEGDE, HCl, NH_4OH, NaOH, acetic acid, and $Cd(NO_3)_2$. Otherwise stated, all used chemicals were analytical grade and purchased from Sigma-Aldrich (Selangor, Malaysia). Iron sand was collected from a local beach in Aceh, Indonesia. Chitosan (C0831 with deacetylation degree of 75.0–85.0%) was procured from Tokyo Chemical Industry co. Ltd. Japan.

2.2 Fe_3O_4 Isolation from iron Sand

Local iron sand was washed with hot water, dried and 15 g was added to a glass beaker containing 100 mL of HCl (12 M). The mixture was stirred at 70 °C for 30 min, cooled to room temperature, and filtered using a filter paper. NH_4OH ($\pm$ 2 mL) was dropped into the solution while stirring at 70 °C for 30 min until a black precipitate was formed. The black precipitate (Fe_3O_4) was dried in an oven at 70 °C for 2 h.

2.3 Preparation of PEDGE-MCh Microspheres
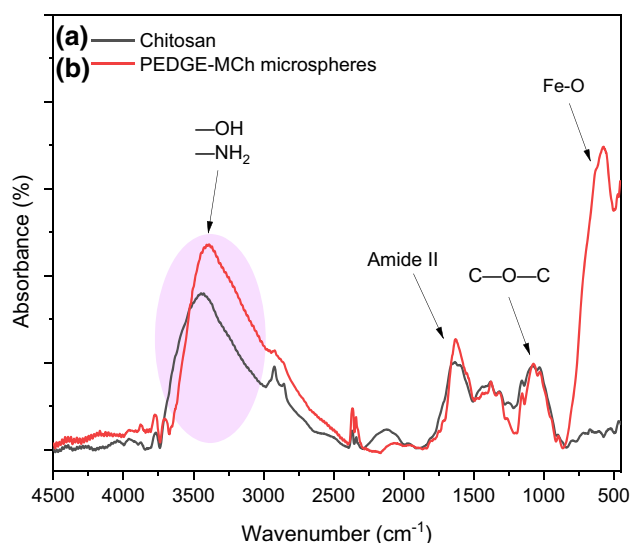
Chitosan (0.35 g) was added to 20 mL of acetic acid (2%) and stirred for 2h at room temperature. PEDGE (0.07 g) was added to the acidic chitosan solution and stirred for a further 2h. To the cross-linked chitosan solution, Fe_3O_4 (0.5 g) was added and stirred for another 1 h. The mixture was then added to a syringe and dropped into 250 mL NaOH (3 M) to form PEDGE cross-linked magnetic chitosan (PEDGE-MCh) microspheres. The obtained PEDGE-MCh microspheres were filtered and washed with distilled water until neutral pH was reached. The PEDGE-MCh microspheres were dried overnight at 40 °C. The PEDGE-MCh microspheres were characterized using Shimadzu XRD-700 Series X-Ray Diffractometer (Kyoto, Japan), Shimadzu FT-IR 8400 (Kyoto, Japan), and SEM-EDS (Jeol. Jsm-6510 LA, Tokyo, Japan), as described in details previously [22].

2.4 Batch Adsorption

The PEDGE-MCh microspheres (0.1 g) were placed in an Erlenmeyer flask containing 25 mL of cadmium solution (25 mg/L). The mixture was shaken at a constant speed of 150 rpm for various contact times (5, 10, 15, 20, 25, 30, 35, 40, 45, and 50 min). After an adsorption process, the adsorbent was separated from the mixture. The cadmium concentration in the solution was determined by a UV–Vis spectrophotometer. The adsorption was also conducted under different pH (2–8) and initial concentrations of cadmium. The solution pH was adjusted with NaOH and HCl before the adsorption process. The initial concentration of Cd^{2+} was varied from 25 to 85 mg/L.

2.5 Adsorption Regeneration

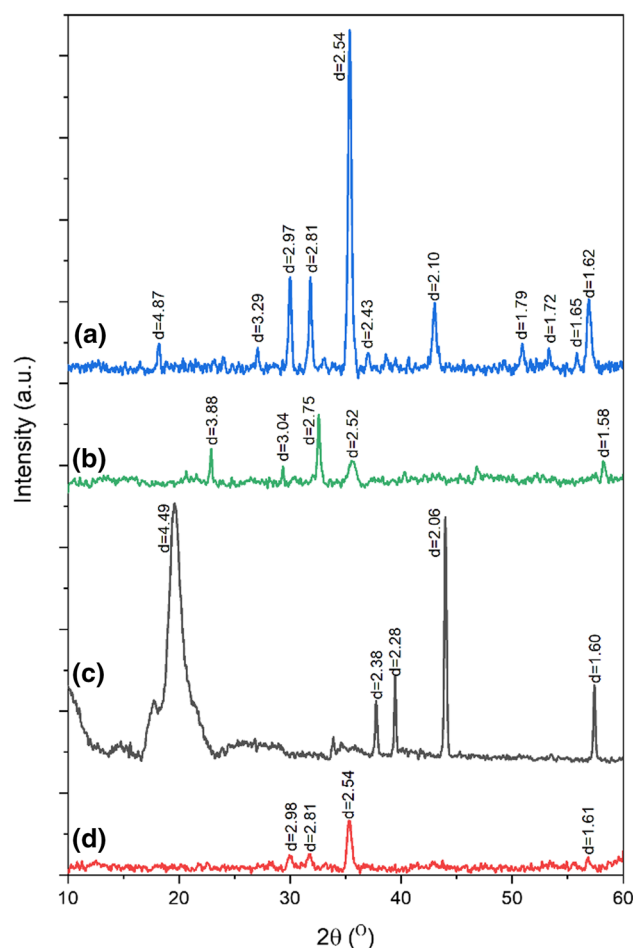0.1 gram of the used PEDGE-MCh microspheres was immersed in 250 mL HNO_3 solution (1.0 mM), shaken and

Fig. 1 FT-IR spectra of chitosan (**a**) and PEDGE-MCh microspheres (**b**)

Fig. 2 X-ray diffraction patterns of iron sand (**a**), iron oxide (**b**), chitosan microspheres (**c**), and PEDGE-MCh microspheres (**d**). Value of d represents the distance from one plane of atoms to another (Å). The diffractograms had been processed with subtracted baseline and smoothed signal using OriginPro 2019b (Northampton, MA, USA)

separated from the solution. The used PEDGE-MCh microspheres were then rinsed until neutral pH was reached and dried overnight at 40 °C. The regenerated PEDGE-MCh microspheres were used again for the adsorption process. The same procedure was conducted for several cycles.

3 Results and Discussion

3.1 FT-IR

FT-IR analysis was performed to study the functional groups of PEDGE-MCh microspheres. The results of FT-IR analysis are shown in Fig. 1. A broad absorption band at wave number 3427 cm^{-1} in chitosan corresponds to overlapping –OH and –NH_2 vibrations. Furthermore, the absorption band at wave number 1633 cm^{-1} is assigned to amide II vibration. The absorption band at 1078 cm^{-1} corresponds to ether (C–O–C) vibration of chitosan. After modification with PEDGE and Fe_3O_4 nanoparticles, the absorption band intensity of –OH vibration increased due to cross-linking that occurred between –NH_2 functional groups from chitosan and epoxide functional groups from PEDGE formed new –OH functional groups. Absorption band intensity of ether vibration also increased due to the presence of same functional group from PEDGE. These results confirmed the formation of cross-linking in chitosan polymer chains by PEDGE. A new absorption band was observed at wave number 582 cm^{-1} corresponding to Fe–O stretching vibration, suggesting the successful embedment. In addition, the shifting of certain absorption bands of chitosan to lower wavenumbers

was observed due to physical interaction among components in the material.

3.2 XRD

XRD patterns of the local iron sand, isolated Fe_3O_4, chitosan, and PEDGE-MCh are presented in Fig. 2. The local iron sand was exhibited to contain Fe_3O_4 magnetite through the appearance of multiple crystalline peaks at $2\theta= 30.06$, 35.38, 43.04 and 56.84° (Fig. 2a). XRD peak observed at $2\theta=31.84°$ corresponds to the crystalline lattice of Fe_2O_3 maghemite. Following the isolation process, the presence of Fe_3O_4 nanoparticles is indicated by its diffractogram patterns at $2\theta=35.52$ and 58.18° (Fig. 2b). The presence of Fe_2O_3 maghemite is still observable at $2\theta=32.58°$. The identification of XRD patterns of Fe_3O_4 and Fe_2O_3 was according to the Joint Committee on Powder Diffraction Standards (JCPDS) number 19-0629 and 39-1346, respectively. To

determine the change of its crystalline property, we employed a calculation of crystalline index based on the entire diffractogram using the previously reported method [23, 24]. We found that the untreated iron sand had higher crystallinity index (52.14%) in comparison with that of the isolated Fe_3O_4 nanoparticles (23.67%). The reduced crystallinity could be seen from lower intensities of diffractogram peaks of Fe_3O_4 nanoparticles than that of iron sand, which is in line to a previously published study [25].

Figure 2c represents the XRD pattern of chitosan, showing a strong typical peak at $2\theta=19.62°$ (Fig. 2c). Other crystalline peaks at $2\theta=37.8$, 39.5, 43.98, and 57.4° also correspond to the crystalline lattice of chitosan but with lower intensities. Upon its modification with PEDGE and Fe_3O_4 nanoparticles (Fig. 2d), most of the crystalline peaks experienced intensities reduction. Several peaks that are observable include those appear at $2\theta=29.94$, 31.84, and 35.22, and 56.84° which confirm the successful immobilization of Fe_3O_4 nanoparticles. Crystallinity indices of chitosan and PEDGE-MCh were obtained 78.08 and 25.52%, respectively. A dramatic reduction in crystallinity was due to the cross-linking and intercalation of Fe_3O_4 nanoparticles among chitosan polymer chains. Cross-linking prevents the mobility of chitosan polymer chains to form crystallite phase at the inversion process of chitosan from liquid to a solid phase [26]. This amorphous material is favorable for the adsorption process due to the high accessibility of adsorbate to reach active sites of the adsorbent [27].

3.3 SEM–EDS

SEM analysis was conducted to study the morphology of materials. SEM image of Fe_3O_4 confirms the presence of polydispersed nanoparticles of various sizes (Fig. 3a). Some particles formed aggregates contributing to larger particle sizes. SEM images of PEDGE-MCh microsphere with different magnifications are presented in Fig. 3b, c. Figure 3b shows the image of PEDGE-MCh microsphere at 100× magnification. The size of PEDGE-MCh microsphere was about 900 μm. Fe_3O_4 nanoparticles used as a filler of chitosan matrix were not observed on the microsphere's surface due to the covering by chitosan polymer (Fig. 3c). The surface of the PEDGE-MCh microsphere was rough, probably due to the existence of Fe_3O_4 nanoparticles inside the chitosan and drying process. Similar SEM appearances of materials after the addition of fillers have been reported previously [3, 22, 28].

EDS spectrum of the PEDGE-MCh microsphere is presented in Fig. 3d. Elemental composition of PEDGE-MCh microsphere (Fig. 3e) suggested the dominance of C and

Element	Weight (%)	Atomic (%)
C	46.06	58.89
O	37.95	36.43
Si	0.86	0.47
Ti	1.02	0.33
Fe	14.12	3.88
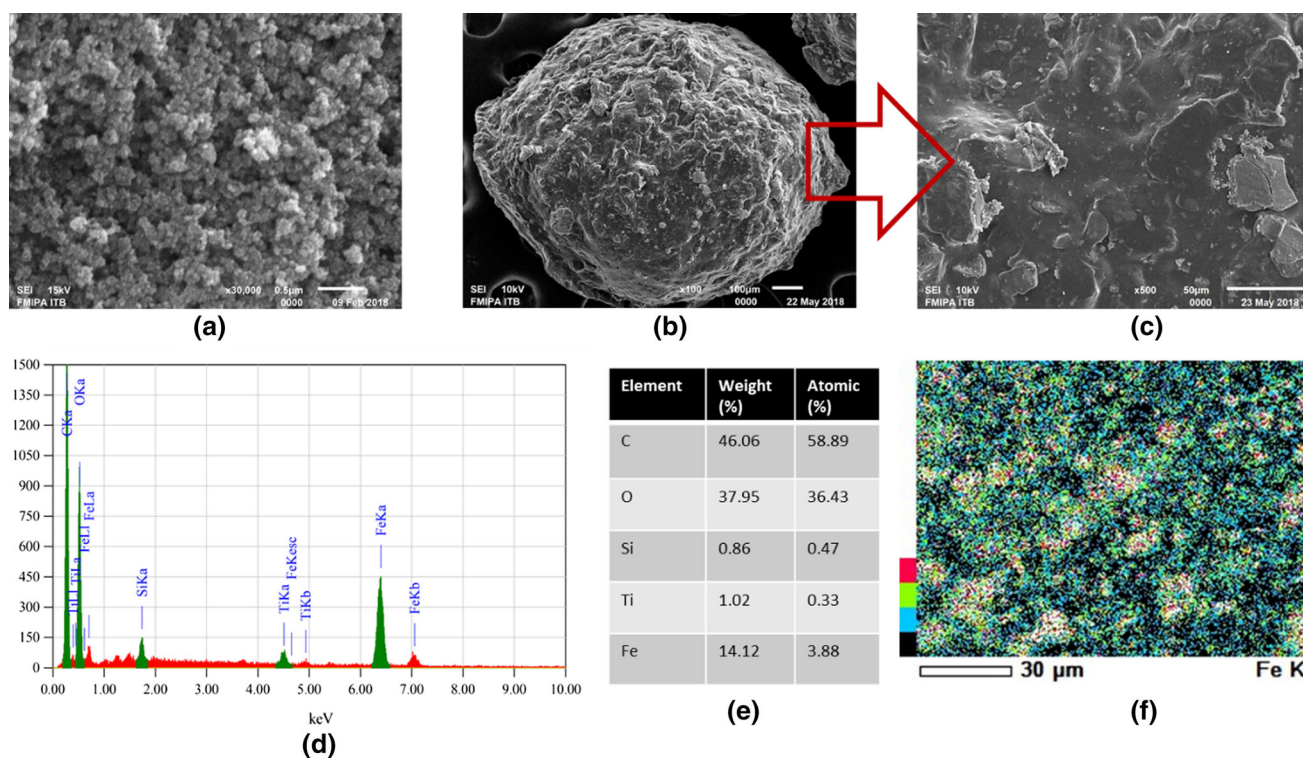
Fig. 3 SEM images of Fe_3O_4 nanoparticles (**a**) and PEDGE-MCh microsphere at 100× (**b**) and 500× (**c**) magnifications. Area EDS spectrum (**d**) with elements and their weight and atomic percentages have been enlisted in a table (**e**). Elemental mapping of Fe (**f**) on the surface of PEDGE-MCh microsphere
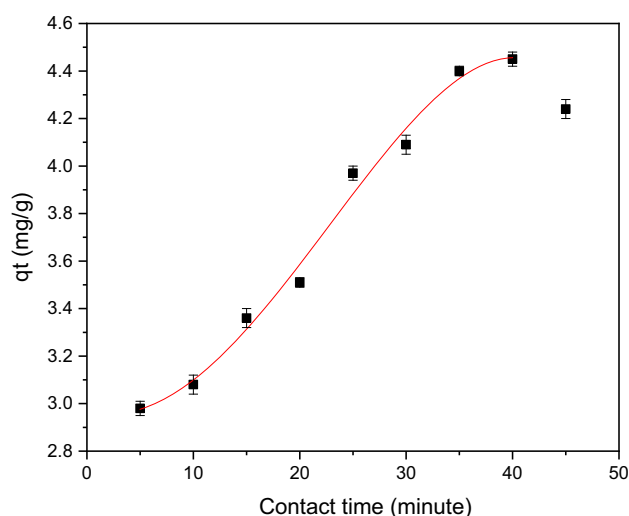
Fig. 4 Influence of contact time on adsorption capacity of Cd^{2+} by PEDGE-MCh microsphere

O which are typical for organic material. Among the metal elements detected (Si, Ti, and Fe), the highest weight percentage was shown by Fe (14.12%). It confirmed the successful embedment of magnetic Fe particles within the PEDGE-MCh microsphere. Further analysis with elemental mapping revealed that the Fe particles had been distributed covering the entire surface of the microsphere (Fig. 3f).

3.4 Adsorption Studies

3.4.1 Contact Time

Several factors influence the adsorption capacity of an adsorbent, such as contact time, solution pH, and concentration of adsorbate. In this work, in order to study the influence of contact time, the adsorption experiments were conducted for several contact times (5, 10, 15, 20, 25, 30, 35, 40, 45, and 50 min). Figure 4 shows the adsorption capacity of Cd^{2+} by PEDGE-MCh microspheres with several contact times. At initial phase, the increase in adsorption capacity was contact time dependent. The adsorption capacity under 10 minutes did not increase significantly, assumed to be associated with the low swelling of chitosan polymer. The chitosan swelling allows more diffusion of adsorbate to the adsorbent surface [29–31]. Later, the adsorption increased in linear correlation due to increased adsorbate diffusion concomitant to the swelling, and the optimum contact time was recorded at around 40 minutes. A decrease in adsorption capacity afterward was due to the detachment of iron oxide particles. It might be attributed to the physical force of the liquid rotation and over-swelling of the chitosan that detached the physically attached iron oxide particles.

3.4.2 pH

In order to study the influence of pH on the adsorption of Cd^{2+} onto PEDGE-MCh, the adsorption experiments were conducted with initial pH variations (pH 2–8). The results are presented in Fig. 5a, where the highest adsorption capacity was obtained at pH 5. At low pH, Cd^{2+} is more likely to be repelled by amino groups protonation-induced electrostatic repulsion. Moreover, at low pH range, Cd^{+2} competes with H^+ ions to bind onto the PEDGE-MCh microspheres. At pH 5, the surface was more negatively charged, becoming electrostatically favorable for Cd^{2+} ions. This phenomenon is induced by the deprotonation of the chitosan surface, as suggested previously [21]. The role of electrostatic interaction of adsorbate-adsorbent was further confirmed by the point of zero charge pH (pH_{pzc}) of PEDGE-MCh microspheres calculated from pH drift method, as used by other reported studies [22, 24]. The pH_{pzc} of PEDGE-MCh adsorbent was obtained pH 5.29 (Fig. 5b). When the pH level of the solution was lower than the pH_{pzc}, the material would form positive charge. Since the adsorbate (Cd^{2+}) has a positive charge, its interaction with the adsorbent would be preferable at higher pH level. Nonetheless, we observed a declining pattern of Cd^{2+} removal efficiency when the pH was increased to be more than pH 5. This occurrence could be associated with the reduced mobility of chitosan polymeric chains at alkaline pH range [29–31], in which the polymer was unable to sufficiently swell to allow more access for Cd^{2+} to reach the binding sites. This finding is in line with a previous report that has thoroughly studied the effect of pH against the chitosan swelling [24].

3.4.3 Adsorption Isotherm

Interaction between the adsorbate and the adsorbent is dependent to the initial concentration. Hence, isotherm modeling could be used to predict the adsorption outcome by plotting the adsorption capacity (q_e) and final concentration at equilibrium (C_e). Herein, we employed the two-parameters isotherm model, Freundlich, and three-parameters isotherm model, Redlich–Peterson. Langmuir isotherm model was not used as the model requires the adsorption to reach equilibrium. Freundlich isotherm model equation is based on the assumption that the adsorbate could form a multilayer adsorption, where the surface energy of each binding site is heterogenous [32]. The Freundlich isotherm model shows a good correlation by $R^2 = 0.9292$ and root-mean-square errors (RMSE) $= 0.661$ (Table 1). However, Redlich–Peterson isotherm model has a better fit with the experimental data ($R^2 = 0.9996$; RMSE $= 0.064$). Therefore, the Redlich-Peterson isotherm model best predicts the adsorption outcome of Cd^{2+} adsorption onto the PEDGE-MCh microsphere. The Redlich–Peterson itself is constructed by the features applied
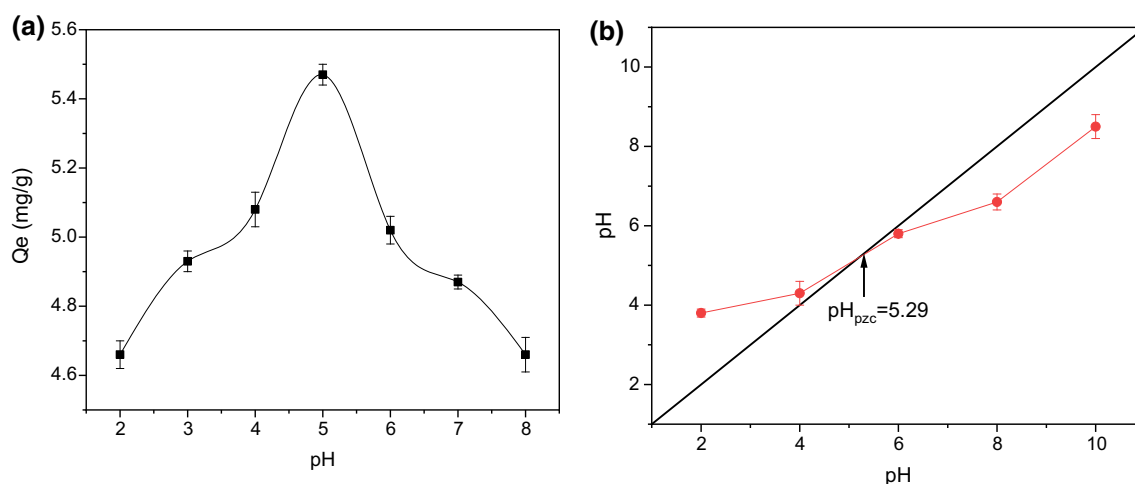
Fig. 5 Influence of initial pH on adsorption capacity of Cd^{2+} by PEDGE-MCh microspheres (**a**). Point of zero charge pH (pH_{pzc}) of PEDGE-MCh microspheres obtained from pH drift method (**b**)

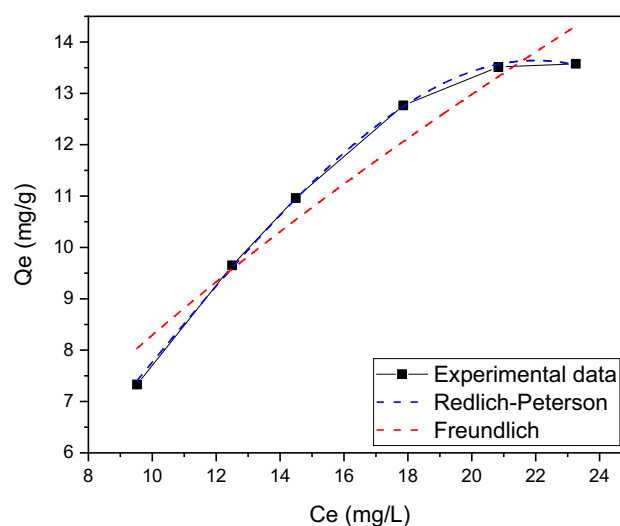**Table 1** The isotherm modeling equations and parameter values

Isotherm models	Parameter	
Freundlich	R^2	0.9292
$q_e = K_F C_e^{1/n}$	RMSE	0.661
	K_F	1.87
	n	1.55
Redlich-Peterson	R^2	0.9996
$q_e = \frac{K_R C_e}{1 + a_R C_e^g}$	RMSE	0.064
	K_R	33.36
	a_R	17.08
	g	0.36

K_F: Freundlich isotherm constant (mg/g) $(dm^3/g)^n$ related to adsorption capacity; n: adsorption intensity; K_R: Redlich–Peterson isotherm constant (L/g); a_R: Redlich–Peterson isotherm constant (1/mg); g: isotherm exponent in Redlich–Peterson model

Fig. 6 Isotherm modeling constructed based on the nonlinear equation of Redlich–Peterson and Freundlich

in Langmuir and Freundlich isotherm model. The isotherm model has superiority in a wide range concentration of pollutant with versatility against homogenous or heterogenous system [33, 34]. The isotherm exponent g that is close to one suggests the adsorption is closely represented by the assumption of Freundlich model where the adsorbate-adsorbent interaction occurs on heterogenous surface in multilayer fashion (Fig. 6).

3.4.4 Adsorption Mechanism

To understand the role of functional group in the adsorption mechanism of Cd^{2+} onto PEDGE-MCh microspheres, FT-IR analysis was conducted on the adsorbent before and after the adsorption, where the results have been presented (Fig. 7). In this part of the study, the batch adsorption was carried
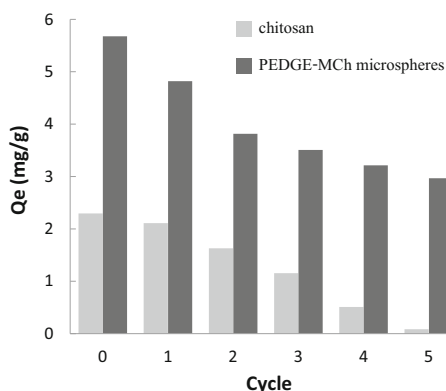
out at pH 7 (neutral) with 45-min contact time. Alterations of the spectral profile before and after the adsorption were observed at around 1381 and 1087 cm^{-1} which correspond to the stretching vibrations of O–C and C–N, respectively. This finding strengthens the claim that both O– and N–containing functional groups are playing significant role in Cd^{2+} adsorption [35, 36]. In previous report, EDTA-modified chitosan could form a complex interaction with Cd^{2+} [22], observed from a new emergence of spectral peak at around 1382 cm^{-1}. Interestingly, in this present study, such phenomenon did not occur, suggesting the adsorption was dependent to electrostatic interaction. The change of spectral profile is observable at a range of 3600–3500 cm^{-1}, where after the adsorption, the intensity and width of the absorption band are found increased. Those phenomena could be associated with the
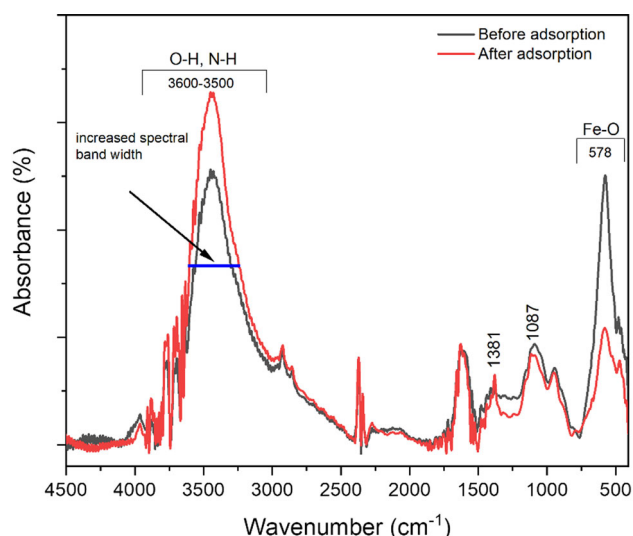
Fig. 7 FT-IR spectra of PEDGE-MCh analyzed before and after the adsorption of Cd^{2+}. The adsorption was carried out at pH 7 for 45 min

the adsorption capacity of PEDGE-MCh fell up to 15.14% from the initial adsorption capacity, which was higher than that of chitosan (8.06%). It is ascribed to the detachment of iron oxide particles from the PEDGE-chitosan matrix. As the adsorbents underwent five cycles of regeneration, the depletion percentage of the adsorption capacity was found higher in chitosan (96.3% from initial adsorption capacity) than that in PEDGE-MCh. It is owing to less iron oxide particles detached from the matrix. Poorer Cd^{2+} adsorption onto chitosan after the 5th cycle could be attributed to the loss of active sites as reported previously [26]. As a distinction, our previous work used the adsorbent in a shape of film with activated carbon acting as the filler, which is completely different to this present study using bead adsorbents with magnetic fillers. Taken altogether, it proves that regeneration is still a challenging factor for PEDGE-cross-linked chitosan adsorbents prepared in our works.

Fig. 8 The adsorption capacity of Cd2 + by chitosan and PEDGE-MCh microspheres for five cycles of regeneration

4 Conclusions

PEDGE-MCh microspheres with a high adsorption capacity of Cd^{2+} ions had been prepared and characterized using FT-IR, XRD, and SEM-EDS. The adsorption was influenced by operating parameters such as contact time and pH, associated with the physical and chemical properties of chitosan. The adsorption of Cd^{2+} ions on PEDGE-MCh microspheresis had the best fitness with Redlich–Peterson isotherm model. PEDGE-MCh microspheres could be used several times, although maintaining the removal efficiency is still a challenging factor.

introduction of new hydroxyl deriving from the adsorbed $Cd(OH)^+$ species. A spectral peak corresponding to the Fe–O stretching vibration ($578\ cm^{-1}$) was observed lower after the adsorption, suggesting the detachment of Fe_3O_4 nanoparticle from the chitosan matrix. It confirms our previous finding, where after the 45-min contact time, the UV–Vis absorbance increased leading to the error of analyzing the real value of Cd^{2+} removal. To enhance the ability of chitosan matrix in immobilizing the Fe_3O_4 nanoparticle, several modifications are suggested including the grafting with amino acids [24, 37].

3.4.5 Regeneration

In this work, adsorbent regeneration was also studied to support the circular economy. The results of regeneration until five cycles have been presented (Fig. 8). At the first cycle,

Declarations

Conflict of interest The authors delcare that they have no conflict of interest.

Consent for Publication All authors have read and agreed to the submitted version of the manuscript.

References

1. Pires, C.T.G.V.M.T.; Vilela, J.A.P.; Airoldi, C.: The effect of chitin alkaline deacetylation at different condition on particle properties. Procedia Chem. **9**, 220–225 (2014). https://doi.org/10.1016/j.proche.2014.05.026

2. Younes, I.; Rinaudo, M.: Chitin and chitosan preparation from marine sources. Structure properties and applications. Mar. Drugs **13**, 1133–1174 (2015). https://doi.org/10.3390/md13031133

3. Safitri, E.; Humaira, H.; Murniana, M.; Nazaruddin, N.; Iqhrammullah, M.; Md Sani, N.D.; Esmaeili, C.; Susilawati, S.; Mahathir, M.; Latansa Nazaruddin, S.: Optical pH sensor based on immobilization anthocyanin from Dioscorea alata L. onto polyelectrolyte complex pectin-chitosan membrane for a determination method of salivary pH. Polymers (Basel) **13**, 1276 (2021). https://doi.org/10.3390/polym13081276

4. Kyzas, G.; Bikiaris, D.: Recent modifications of chitosan for adsorption applications: a critical and systematic review. Mar. Drugs **13**, 312–337 (2015). https://doi.org/10.3390/md13010312

5. Jayanudin, J.; Rochmadi, R.; Fahrurrozi, M.; Wirawan, S.: Microencapsulation technology of ginger oleoresin with chitosan as wall material: a review. J. Appl. Pharm. Sci. **6**(12), 209–223 (2016). https://doi.org/10.7324/JAPS.2016.601232

6. Song, Z.; Li, G.; Guan, F.; Liu, W.: Application of chitin/chitosan and their derivatives in the papermaking industry. Polymers (Basel) **10**, 389 (2018). https://doi.org/10.3390/polym10040389

7. Vakili, M.; Rafatullah, M.; Salamatinia, B.; Abdullah, A.Z.; Ibrahim, M.H.; Tan, K.B.; Gholami, Z.; Amouzgar, P.: Application of chitosan and its derivatives as adsorbents for dye removal from water and wastewater: a review. Carbohydr. Polym. **113**, 115–130 (2014). https://doi.org/10.1016/j.carbpol.2014.07.007

8. Fan, C.; Li, K.; He, Y.; Wang, Y.; Qian, X.; Jia, J.: Evaluation of magnetic chitosan beads for adsorption of heavy metal ions. Sci. Total Environ. **627**, 1396–1403 (2018). https://doi.org/10.1016/j.scitotenv.2018.02.033

9. Iqhrammullah, M.; Mustafa, I.: The application of Chitosan modified polyurethane foam adsorbent. RASĀYAN J. Chem. **12**, 494–501 (2019). https://doi.org/10.31788/RJC.2019.1225080

10. Sobahi, T.R.A.; Abdelaal, M.Y.; Makki, M.S.I.: Chemical modification of Chitosan for metal ion removal. Arab. J. Chem. **7**, 741–746 (2014). https://doi.org/10.1016/j.arabjc.2010.12.011

11. Islam, S.; Bhuiyan, M.A.R.; Islam, M.N.: Chitin and Chitosan: structure, properties and applications in biomedical engineering. J. Polym. Environ. **25**, 854–866 (2017). https://doi.org/10.1007/s10924-016-0865-5

12. Gutha, Y.; Zhang, Y.; Zhang, W.; Jiao, X.: Magnetic-epichlorohydrin crosslinked chitosan schiff's base (m-ECCSB) as a novel adsorbent for the removal of Cu(II) ions from aqueous environment. Int. J. Biol. Macromol. **97**, 85–98 (2017). https://doi.org/10.1016/j.ijbiomac.2017.01.004

13. Kildeeva, N.R.; Perminov, P.A.; Vladimirov, L.V.; Novikov, V.V.; Mikhailov, S.N.: About mechanism of chitosan cross-linking with glutaraldehyde. Russ. J. Bioorgan. Chem. **35**, 360–369 (2009). https://doi.org/10.1134/S106816200903011X

14. Mirzaei, B.E.; Ramazani, S.A.A.; Shafiee, M.; Danaei, M.: Studies on glutaraldehyde crosslinked chitosan hydrogel properties for drug delivery systems. Int. J. Polym. Mater. **62**, 605–611 (2013). https://doi.org/10.1080/00914037.2013.769165

15. Zhang, X.; Jin, X.; Xu, C.; Shen, X.: Preparation and characterization of glutaraldehyde crosslinked chitosan nanofiltration membrane. J. Appl. Polym. Sci. **128**, 3665–3671 (2013). https://doi.org/10.1002/app.38580

16. Jozwiak, T.; Filipkowska, U.; Rodziewicz, J.; Nowosad, E.: Effect of cross-linking with glutaraldehyde on adsorption capacity of chitosan beads. Prog. Chem. Appl. Chitin Deriv. **28**, 35–48 (2013)

17. Kyzas, G.Z.; Deliyanni, E.A.: Mercury removal with modified magnetic Chitosan adsorbents. Molecules **18**, 6193–6214 (2013)

18. Zhao, W.; Huang, X.; Wang, Y.; Sun, S.; Zhao, C.: A recyclable and regenerable magnetic chitosan absorbent for dye uptake. Carbohydr. Polym. **150**, 201–208 (2016). https://doi.org/10.1016/j.carbpol.2016.05.037

19. Liu, Z.; Wang, H.; Liu, C.; Jiang, Y.; Yu, G.; Mu, X.; Wang, X.: Magnetic cellulose–chitosan hydrogels prepared from ionic liquids as reusable adsorbent for removal of heavy metal ions. Chem. Commun. **48**, 7350 (2012). https://doi.org/10.1039/c2cc17795a

20. Zhang, X.; Sun, C.; Zhang, L.; Liu, H.; Cao, B.; Liu, L.; Gong, W.: Adsorption studies of cadmium onto magnetic Fe3O4@FePO4 and its preconcentration with detection by electrothermal atomic absorption spectrometry. Talanta **181**, 352–358 (2018). https://doi.org/10.1016/j.talanta.2018.01.023

21. Alizadeh, B.; Delnavaz, M.; Shakeri, A.: Removal of Cd(II) and phenol using novel cross-linked magnetic EDTA/chitosan/TiO2 nanocomposite. Carbohydr. Polym. **181**, 675–683 (2018). https://doi.org/10.1016/j.carbpol.2017.11.095

22. Iqhrammullah, M.; Audina, U.; Husin, H.; Fathana, H.: Adsorptive removal of Cd (II) using oil palm empty fruit bunch-based charcoal/chitosan-EDTA film composite. Sustain. Chem. Pharm. **21**, 100449 (2021). https://doi.org/10.1016/j.scp.2021.100449

23. Rahmi, R.; Lubis, S.; Az-Zahra, N.; Puspita, K.; Iqhrammullah, M.: Synergetic photocatalytic and adsorptive removals of metanil yellow using TiO2/grass-derived cellulose/chitosan (TiO2/GC/CH) film composite. Int. J. Eng. **34**, 1827–1836 (2021). https://doi.org/10.5829/ije.2021.34.08b.03

24. Nina, M.; Fathana, H.; Iqhrammullah, M.: Preparation and characterization of new magnetic chitosan-glycine-PEGDE (Fe3O4/Ch-G-P) beads for aqueous Cd(II) removal. J. Water Process Eng. **45**, 102493 (2022). https://doi.org/10.1016/j.jwpe.2021.102493

25. Zein, I.; Jalil, Z.: Identification of magnetite material (Fe3O4) based on natural materials as catalyst for industrial raw material application. J. Phys. Conf. Ser. **1232**, 012054 (2019). https://doi.org/10.1088/1742-6596/1232/1/012054

26. Nurfatimah, R.: Preparation of polyethylene glycol diglycidyl ether (PEDGE) crosslinked chitosan/activated carbon composite film for Cd2+ removal. Carbohydr. Polym. **199**, 499–505 (2018). https://doi.org/10.1016/J.CARBPOL.2018.07.051

27. Hameed, A.M.: Synthesis of Si/Cu amorphous adsorbent for efficient removal of methylene blue dye from aqueous media. J. Inorg. Organomet. Polym. Mater. **30**, 2881–2889 (2020). https://doi.org/10.1007/s10904-019-01436-1

28. Iqhrammullah, M.; Saleha, S.; Maulina, F.P.; Idroes, R.: Polyurethane film prepared from ball-milled algal polyol particle and activated carbon filler for NH3–N removal. Heliyon **6**, e04590 (2020). https://doi.org/10.1016/j.heliyon.2020.e04590

29. Nagarpita, M.V.; Roy, P.; Shruthi, S.B.; Sailaja, R.R.N.: Synthesis and swelling characteristics of chitosan and CMC grafted sodium acrylate-co-acrylamide using modified nanoclay and examining its efficacy for removal of dyes. Int. J. Biol. Macromol. **102**, 1226–1240 (2017). https://doi.org/10.1016/j.ijbiomac.2017.04.099

30. Trikkaliotis, D.G.; Christoforidis, A.K.; Mitropoulos, A.C.; Kyzas, G.Z.: Adsorption of copper ions onto chitosan/poly(vinyl alcohol) beads functionalized with poly(ethylene glycol). Carbohydr. Polym. **234**, 115890 (2020). https://doi.org/10.1016/j.carbpol.2020.115890

31. Ibrahim, A.G.; Sayed, A.Z.; Abd El-Wahab, H.; Sayah, M.M.: Synthesis of a hydrogel by grafting of acrylamide-co-sodium methacrylate onto chitosan for effective adsorption of Fuchsin basic dye. Int. J. Biol. Macromol. **159**, 422–432 (2020). https://doi.org/10.1016/j.ijbiomac.2020.05.039

32. Freundlich, H.M.F.: Over the adsorption in solution. J. Phys. Chem. **57**, 385–471 (1906)

33. Foo, K.Y.; Hameed, B.H.: Insights into the modeling of adsorption isotherm systems. Chem. Eng. J. **156**, 2–10 (2010). https://doi.org/10.1016/j.cej.2009.09.013

34. Al-Ghouti, M.A.; Da'ana, D.A.: Guidelines for the use and interpretation of adsorption isotherm models: a review. J. Hazard. Mater. **393**, 122383 (2020). https://doi.org/10.1016/j.jhazmat.2020.122383

35. Iqhrammullah, M.; Suyanto, H.; Pardede, M.; Karnadi, I.; Kurniawan, K.H.; Chiari, W.; Abdulmadjid, S.N.: Cellulose acetate-polyurethane film adsorbent with analyte enrichment for in-situ detection and analysis of aqueous Pb using Laser-Induced Breakdown Spectroscopy (LIBS). Environ. Nanotechnol. Monit. Manag. **16**, 100516 (2021). https://doi.org/10.1016/j.enmm.2021.100516

36. Yin, W.; Zhao, C.; Xu, J.; Zhang, J.; Guo, Z.; Shao, Y.: Removal of Cd(II) and Ni(II) from aqueous solutions using activated carbon developed from powder-hydrolyzed-feathers and Trapa natans husks. Colloids Surf. A Physicochem. Eng. Asp. **560**, 426–433 (2019). https://doi.org/10.1016/J.COLSURFA.2018.10.031

37. Fathana, H.; Iqhramullah, M.; Rahmi, R.; Adlim, A.; Lubis, S.: Tofu wastewater-derived amino acids identification using LC-MS/MS and their uses in the modification of chitosan/TiO2 film composite. Chem. Data Collect. **35**, 100754 (2021). https://doi.org/10.1016/j.cdc.2021.100754